The effects of dynamic compression on the development of cartilage grafts engineered using bone marrow and infrapatellar fat pad derived stem cells

Lu Luo[1,2], Stephen Thorpe[3], Conor T. Buckley[1,2], Daniel J. Kelly[1,2,4,5]*

[1]Trinity Centre for Bioengineering, Trinity Biomedical Sciences Institute, Trinity College Dublin, Dublin, Ireland.

[2]Department of Mechanical and Manufacturing Engineering, School of Engineering, Trinity College Dublin, Dublin, Ireland.

[3]School of Engineering and Materials Science, Queen Mary University of London, United Kingdom.

[4]Department of Anatomy, Royal College of Surgeons in Ireland, Dublin 2, Ireland.

[5]Advanced Materials and Bioengineering Research Centre (AMBER), Royal College of Surgeons in Ireland and Trinity College Dublin, Dublin, Ireland.

*Corresponding author

E-mail address: kellyd9@tcd.ie

Address: Department of Mechanical and Manufacturing Engineering

School of Engineering

Trinity College Dublin

Dublin 2

Ireland

Telephone: +353-1-896-3947

Fax: +353-1-679-5554

Abstract

Bioreactors that subject cell seeded scaffolds or hydrogels to biophysical stimulation have been used to improve the functionality of tissue engineered cartilage and to explore how such constructs might respond to the application of joint specific mechanical loading. Whether a particular cell type responds appropriately to physiological levels of biophysical stimulation could be considered a key determinant of its suitability for cartilage tissue engineering applications. The objective of this study was to determine the effects of dynamic compression on chondrogenesis of stem cells isolated from different tissue sources. Porcine bone marrow (BM) and infrapatellar fat pad (FP) derived stem cells were encapsulated in agarose hydrogels and cultured in a chondrogenic medium in free swelling (FS) conditions for 21 days, after which samples were subjected to dynamic compression (DC) of 10% strain (1Hz, 1 hour/day) for a further 21 days. Both BM derived stem cells (BMSCs) and FP derived stem cells (FPSCs) were capable of generating cartilaginous tissues with near native levels of sulfated glycosaminoglycan (sGAG) content, although the spatial development of the engineered grafts strongly depended on the stem cell source. The mechanical properties of cartilage grafts generated from both stem cell sources also approached that observed in skeletally immature animals. Depending on the stem cell source and the donor, the application of DC either enhanced or had no significant effect on the functional development of cartilaginous grafts engineering using either BMSCs or FPSCs. BMSC seeded constructs subjected to DC stained less intensely for collagen type I. Furthermore, histological and micro-computed tomography analysis showed mineral deposition within BMSCs seeded constructs was suppressed by the application of DC. Therefore, while the application of DC *in vitro* may only lead to modest improvements in the mechanical functionality of cartilaginous grafts, it may play an important role in the development of phenotypically stable constructs.

Introduction

Adult stem cells represent a promising cell source for cartilage tissue engineering, due to their chondrogenic potential and rapid self-renewing ability. They have been identified in various tissues, such as bone marrow (BM) (Pittenger et al., 1999, Johnstone et al., 1998, Yoo et al., 1998), adipose tissue (Erickson et al., 2002, Gimble and Guilak, 2003, Guilak et al., 2004), infrapatellar fat pad (FP) (Dragoo et al., 2003, Wickham et al., 2003, English et al., 2007) and synovium (Pei et al., 2008, Pei et al., 2009, Vinardell et al., 2012b), among which BM derived stem cells (BMSCs) are perhaps the most extensively studied cell type. Various studies have demonstrated successful chondrogenic induction of BMSCs in a number of different biomaterials, including naturally derived materials (e.g., collagen, hyaluronic acid, alginate, agarose) (Matsiko et al., 2012, Bian et al., 2011, Li et al., 2009, Thorpe et al., 2010) and synthetic materials (e.g., polyglycolic acid (PGA) and polycaprolactone (PCL)) (Kafienah et al., 2007, Wise et al., 2009) among others. In spite of their tremendous promise, there are a number of potential limitations associated with BMSC based tissue engineering strategies for articular cartilage repair. Firstly, it has been demonstrated that cartilage engineered using BMSCs has inferior biochemical and biomechanical properties to that engineered using primary chondrocytes (Erickson et al., 2009, Mauck et al., 2006). Furthermore, studies have also shown that cartilage tissues engineered using BMSCs have the potential to undergo hypertrophy and endochondral ossification (Kafienah et al., 2007, Pelttari et al., 2006). This has motivated the use of alternative stem cell sources for cartilage tissue engineering. Compared to BMSCs, stem cells isolated from the infrapatellar fat pad (FP) of the knee are arguably easier to isolate, with a lower degree of invasiveness and minimal patient morbidity (Dragoo et al., 2003). FP derived stem cells (FPSCs) have successfully been used for engineering cartilaginous tissues (Buckley and Kelly, 2012, Buckley et al., 2010a, Buckley et al., 2010b, Liu et al., 2013, Liu et al., 2012, Jurgens et al., 2009, Felimban et al., 2014, Ye et al., 2014), with such grafts demonstrating at

least comparable functionality to those generated using BMSCs (Vinardell et al., 2011). Furthermore, studies have shown that cartilage grafts engineered using FPSCs have a lower tendency to undergo endochondral ossification compared to those engineered using BMSCs (Vinardell et al., 2012b).

Physiologically, articular cartilage exists in a complex biomechanical environment, being subjected to cyclical deformational loading and large hydrostatic pressures during joint movement (Mow and Wang, 1999). It has been demonstrated that mechanical cues play an important role in the development (Mikic et al., 2000, Mikic et al., 2004), remodeling (Rieppo et al., 2009) and repair of this tissue (Wakitani et al., 1994). More recently, dynamic compression has been explored as a potential stimulus to enhance chondrogenesis for cartilage tissue engineering applications. Numerous studies have demonstrated that dynamic compression can increase cartilage-specific matrix synthesis by chondrocytes (Demarteau et al., 2003, Mauck et al., 2000, Buschmann et al., 1995). Moreover, dynamic compression has also been shown to regulate chondrogenesis of BMSCs at both the gene and protein level (Huang et al., 2005, Haugh et al., 2011, Kelly and Jacobs, 2010, Thorpe et al., 2008, Thorpe et al., 2010, Li et al., 2010a, Li et al., 2010b), with increased sulfated glycosaminoglycan (sGAG) accumulation reported in BMSCs seeded hydrogels following the application of loading (Mauck et al., 2007, Kisiday et al., 2009, Thorpe et al., 2013). Such mechanical stimulation protocols have also been shown to improve the mechanical properties of BMSC seeded cartilage constructs (Huang et al., 2010, Thorpe et al., 2013, Bian et al., 2012).

Understanding how cartilaginous tissues engineered using stem cells will respond to the local mechanical environment will be critical to successful clinical cartilage repair. While a number of studies have shown that dynamic compression can promote chondrogenesis of BMSCs, to the best of our knowledge no study to date has compared the response of stem cells isolated from different tissue sources to this biophysical stimulus. Therefore, the objective of this study was to compare the effects

of dynamic compression on chondrogenesis of BMSCs and FPSCs that were encapsulated in agarose hydrogels. We hypothesized that dynamic compression would enhance the functional development of cartilaginous tissues engineered using stem cells independent of their origin. To test this hypothesis, porcine BMSCs and FPSCs were encapsulated in agarose hydrogels and cultured in the presence of TGF-β3 for 3 weeks before being subjected to dynamic compression of 10% strain (1Hz, 1 hour/day) for a further 3 weeks. We first investigated the temporal and spatial development of cartilage grafts engineered in free swelling culture using stem cells of different origin, and then investigated the influence of dynamic compression on: 1) cartilage specific matrix accumulation and the subsequent mechanical properties of the engineered tissue; 2) the spatial distribution of matrix within the engineered tissue; and 3) the tendency of stem cell seeded cartilage constructs to undergo hypertrophy and to begin to calcify.

Materials and Methods

Cell Isolation and Expansion

Porcine BMSCs were obtained from the bone marrow of the femur and FPSCs from the entire infrapatellar fat pad of the knee joint (n=2, 3-4 months old, ~50kg). The isolation of these cells from porcine donors was approved by the ethics board of Trinity College Dublin (Dublin, Ireland) and the procedures were conducted according to local guidelines. BMSCs were isolated using an adapted protocol used for human BMSCs isolation (Lennon and Caplan, 2006) and FPSCs were isolated as previously described (Buckley and Kelly, 2012). After isolation, BMSCs and FPSCs were seeded at a density of $5x10^3$ cell/cm^2 in high-glucose Dulbecco's modified Eagle's medium (hgDMEM) GlutaMAX™ supplemented with 10% fetal bovine serum and 1% penicillin (100 U/mL)-streptomycin (100 µg/mL) (all GIBCO, Biosciences, Dublin, Ireland) and expanded to passage two (P2) in a humidified atmosphere of 5% CO_2 at 37°C. For both BMSCs and FPSCs, 5 ng/ml fibroblast-growth factor-2 (ProSpec-Tany TechnoGene Ltd, Israel) was added into the medium (from the beginning of P0 for FPSCs; from the beginning of P1 for BMSCs) to promote the growth and chondrogenic potential of stem cells (Buckley and Kelly, 2012).

Hydrogel construct fabrication and culturing

BMSCs and FPSCs (both P2) were encapsulated respectively in agarose (Type VII) as previously described (Thorpe et al., 2010) to obtain a final gel concentration of 2% and a cell density of 30 x 10^6 cells/ml. The agarose-gel suspension was then cast into a stainless steel mold from which cylindrical constructs (Ø6 mm × 4 mm thickness) were removed using a biopsy punch. Constructs were then maintained separately in 6-well-plates in 9 ml of chondrogenic medium (per construct) consisting of hgDMEM

GlutaMAX™ supplemented with penicillin (100 U/ml)-streptomycin (100 µg/ml), 100 µg/ml sodium pyruvate, 40 µg/ml L-proline, 4.7 µg/mL linoleic acid, 50 µg/ml L-ascorbic acid-2-phosphate, 1.5 mg/ml bovine serum albumin, 1 × insulin–transferrin–selenium, 100 nM dexamethasone (all from Sigma-Aldrich, Dublin, Ireland) and 10 ng/ml recombinant human transforming growth factor-β3 (TGF-β3; ProSpec-Tany TechnoGene Ltd). Media was exchanged twice weekly. At each exchange, media was sampled and stored at -85°C for biochemical analysis.

Experimental design

Cell seeded hydrogels (generated using BMSCs and FPSCs) were first maintained in free swelling (FS) conditions in a chondrogenic medium for 21 days to allow differentiation toward a chondrogenic phenotype and matrix establishment (Haugh et al., 2011). At this point, half of the samples were subjected to dynamic compression (DC) of 10% strain (1Hz, 1 hour/day, 5 days/week) for a further 21 days as previously described (Thorpe et al., 2010), while the remaining samples were maintained in FS conditions to serve as a control. We chose this delayed loading protocol, since previous studies have shown that applying DC immediately after cell encapsulation can suppress chondrogenesis of BMSCs, whereas delayed application of DC leads to enhanced chondrogenesis (Thorpe et al., 2010, Thorpe et al., 2013). Constructs (n=6 per group) were assessed at day 0, 21 and 42. This experiment was repeated again using cells isolated from a different donor.

Assessment of mechanical properties

Construct mechanical properties were tested (n=4 per group) using a standard materials testing machine with a 5N load cell (Zwick Roell Z005, Herefordshire, UK) as previously described (Buckley et al., 2009). Briefly, constructs were immersed in phosphate buffered saline (PBS) bath (room temperature) and placed between two impermeable platens. A preload of 0.01 N was used to ensure direct contact between

construct and platen surfaces. An unconfined stress-relaxation test was then performed, which consisted of a ramp compression up to 10% strain of the sample thickness followed by a hold period of 30 minutes until equilibrium was reached. The equilibrium compressive modulus of the sample was calculated from the equilibrium force. A dynamic test consisting of a cyclic strain amplitude of 1% at 1 Hz for 10 cycles was performed directly after the equilibrium test to determine the dynamic modulus.

Quantitative biochemical analysis

Construct analysis

After mechanical testing, constructs were maintained in PBS for 30 mins to allow them to recover to their initial thickness, after which constructs (n=3/4 per group) were transversely sliced into two halves for determination of the spatial distribution of matrix within the engineered tissue. The top and bottom halves of the samples were weighed (wet) and stored separately at -85 °C for subsequent analyses. Samples were digested with 125 μg/ml papain in 0.1 M sodium acetate, 5 mM L-cysteine HCl, 0.05 M EDTA, pH 6.0 (all Sigma-Aldrich) under constant rotation at 60 °C for 18 hours. The DNA content of the samples was measured using the Hoechst bisBenzimide H33258 dye assay with calf thymus DNA as a standard as previously described (Kim et al., 1988). sGAG content was quantified using the dimethylmethylene blue dye-binding assay (Blyscan, Biocolor Ltd., Northern Ireland), with a chondroitin sulfate standard. Collagen content was determined through measurement of the hydroxyproline content (Kafienah and Sims, 2004) and calculated using a hydroxyproline-to-collagen ratio of 1:7.69 (Ignat'eva et al., 2007). Matrix accumulation (sGAG and collagen) were normalized to construct wet weight and to DNA content.

Media analysis

Aliquots sampled at each media exchange from day 21 to day 42 were analyzed for

total sGAG or collagen content secreted into the media during this period using the methods described above. Total medium volume was accounted for and data is presented as average sGAG or collagen content released per construct into media from day 21 to day 42. Media samples from day 21 to day 42 were also analyzed for alkaline phosphatase (ALP) activity using a Sensolyte pNPP Alkaline Phosphatase assay kit (Cambridge Biosciences, UK) with a calf intestine ALP standard (Sheehy et al., 2012).

Histology and immunohistochemistry

Whole constructs (n=2 per group) were fixed with 4% paraformaldehyde (Sigma-Aldrich), wax embedded and sectioned perpendicularly to the disk surface at a thickness of 5 μm. Sections were stained histologically with 1% alcian blue 8GX in 0.1M HCl for sGAG distribution, picrosirius red for collagen distribution and 1% alizarin red for mineral deposition (all Sigma–Aldrich). Sections were also immunohistochemically stained for collagen type I and II using a mouse monoclonal collagen type I antibody (1:100; 1.4 mg/mL; Abcam, Cambridge, UK) and a mouse monoclonal collagen type II antibody (1:80; 1 mg/mL; Abcam) respectively as previously described (Thorpe et al., 2010). Sections of porcine cartilage and ligament were included as controls.

Micro-computed tomography analysis

Constructs (n=2 per group) were scanned using micro-computed tomography (μCT) in order to assess the mineral content and distribution within the samples. Scans were performed using a Scanco Medical μCT 40 system (Scanco Medical, Bassersdorf, Switzerland) at a voltage of 70 kVp and a current of 114 μA. Data is presented as the volume of mineral within each construct. A 3-dimensional (3D) image of the mineral deposition within the constructs was also obtained from the system.

Statistical analysis

Statistics were performed using MINITAB 15.1 software (Minitab Ltd., Coventry, UK). For data where two factors of comparison (day 21 vs. 42 and/or BM vs. FP and/or top vs. bottom and/or FS vs. DC) were required, a general lineal model for analysis of variance with Tukey's test for multiple comparisons was used. For direct comparison between FS and DC group, a two-sample T-test was used. Significance was determined at $p \leq 0.05$ and a trend towards significance was defined as $p \leq 0.1$. All graphical results are presented as mean $\pm$ standard deviation.

Results

Temporal and spatial development of cartilage grafts engineered in free swelling culture using different sources of stem cells

We first investigated the temporal development of cartilaginous constructs engineered using both BM and FP derived stem cells in free swelling (FS) culture. A significant increase in DNA content was observed in FP constructs from day 21 to day 42 ($p<0.05$), indicating cell proliferation, while the DNA content of BM constructs remained relatively constant over the same culture period (Fig. 1A). A significant increase in sGAG and collagen content from day 21 to day 42 was also seen in both BM constructs and FP constructs ($p<0.05$; Fig. 1A). At day 42, the sGAG content in BM constructs was ~2% (w/w), compared to ~3% (w/w) in FP constructs. The collagen content was significantly higher in BM constructs compared to FP constructs ($p<0.05$; Fig. 1A).

Histological staining was used to examine the spatial distribution of matrix within the FS constructs at day 42. Compared to FP constructs, a relatively homogeneous distribution of sGAG and collagen was observed throughout the depth of BM constructs, although the core of the engineered tissue did stain slightly more intensely for glycosaminoglycans (Alcian Blue) and type II collagen (Fig. 1B). This was further confirmed through biochemical quantification of the matrix content in the top and bottom halves of the constructs, with similar levels of DNA, sGAG and collagen observed in the top and bottom of the BM constructs (data not shown). A more heterogeneous distribution of matrix was observed in FP constructs, with decreased sGAG and collagen accumulation through the depth of the engineered tissue (and also from periphery towards core; Fig. 1B). Biochemical data also confirmed a significantly higher level of sGAG and collagen content in the top compared the bottom of FP constructs, although no significant difference in DNA content between

top and bottom of the engineered tissue was observed (data not shown).

Immunohistochemical analysis showed a strong staining for collagen type II in BM constructs at day 42, while a weaker staining was found in FP constructs (Fig. 1B). Positive staining for collagen type I was also observed in the peripheral region of the BM constructs (albeit staining less intensely than for collagen type II). FP constructs stained weakly for collagen type I (Fig. 1B).

In a replicate of this experiment, where BM and FP constructs were fabricated using cells isolated from another donor, similar temporal and spatial matrix development was observed again for each construct type. However, higher sGAG accumulation (~4% (w/w)) was observed in BM constructs engineered using the second donor. The sGAG content in FP constructs engineered using this donor remained ~3% (w/w) (Supplementary Fig. 1).

The influence of dynamic compression on the functional properties of cartilage grafts engineered using different sources of stem cells

To assess the effects of delayed dynamic compression (DC) on chondrogenesis of BM and FP stem cell seeded constructs, samples were first cultured in a chondrogenic medium in FS conditions for 3 weeks (day 0-21) to allow differentiation toward a chondrogenic phenotype and matrix establishment, before subjection to DC for a further 3 weeks (day 21-42). DC lead to a small but statistically significant increase in sGAG ($p<0.05$; Figs. 2B, 2D) and collagen ($p<0.05$; Figs. 2C, 2E) accumulation in BM constructs. For FP constructs, DC didn't significantly alter any of the biochemical constituents of the engineered tissue (Figs. 2 H-L). At day 42, the equilibrium and dynamic modulus of BM constructs maintained in FS culture conditions was ~70 kPa and ~700 kPa respectively (Figs. 2F, 2G); while the equilibrium and dynamic modulus of FP constructs maintained in FS culture conditions was notably higher at ~300 kPa and ~1400 kPa respectively (Figs. 2M, 2N). DC significantly enhanced the

equilibrium and dynamic modulus of BM constructs ($p<0.001$; Figs. 2F, 2G), however it had no significant effect on the mechanical properties of the FP constructs (Figs. 2M, 2N).

sGAG and collagen accumulation within the hydrogels, and that released into medium during the loading period (day 21-42), was also assessed in order to examine the direct influence of DC on absolute levels of extracellular matrix (ECM) synthesis. Higher levels of sGAG release into the medium was observed in BM constructs with the application of loading, such that DC significantly enhanced total amount of sGAG synthesis (accumulated + released) over the loading period ($p<0.01$; Fig. 3A). The total amount of collagen synthesis in BM constructs over this period was, however, not affected by the application of DC (Fig. 3B). For FP constructs, no significant difference in sGAG or collagen synthesis was observed between the FS and DC samples (Figs. 3C, 3D).

In a replicate using stem cells from a different donor, DC was found to have no significant effect on the bulk biochemical composition or the mechanical properties of either BM or FP grafts (supplementary Fig. 2). Similarly, in this experiment DC did not significantly alter the total sGAG or collagen synthesis (accumulated + released) over the loading period (data not shown).

Histological analysis showed no obvious difference in staining intensity for sGAG or collagen, at the macroscopic level, between FS and DC samples for either BM or FP constructs engineered from either donor (Fig. 4 and supplementary Fig. 3). Similarly, DC did not appear to influence collagen type II accumulation. Moderate staining for collagen type I was found in the peripheral region of FS cultured BM constructs engineered from both donors; however, less intense staining was observed in BM constructs subjected to DC for both donors (Fig. 4 and supplementary Fig. 3). FP constructs stained weakly for collagen type I regardless of the loading condition.

The influence of DC on the spatial development of engineered cartilage

Overall, the application of DC did not dramatically alter the spatial accumulation of sGAG or collagen in the top and bottom of engineered tissues (Fig. 5 A-F), although matrix distribution appeared more homogeneous in FP constructs engineered from donor 2 (Fig. 5G, 5H). Histological staining revealed that the peripheral of engineered BM constructs stained weakly for sGAG under FS conditions. The pericellular region of cells in this region of loaded BM constructs appeared to be richer in sGAGs (supplementary Fig. 4).

The influence of DC on hypertrophy of chondrogenically primed BMSCs

Alizarin red staining and μCT scans were carried out to assess mineralization of the engineered cartilaginous constructs. At day 42, positive staining was found in FS cultured BM constructs from both donors, while tissues subjected to DC stained less intensively or negatively (Fig. 6A). Despite this, no significant difference in ALP activity in the media of FS and DC constructs was found (data not shown). μCT scans revealed variable mineral deposition within the constructs (Fig. 6B), and in general less mineral accumulation was observed in DC samples compared to FS controls (Fig. 6C). In contrast, no evidence of mineralization was observed in FP constructs (Fig. 6A). Furthermore, no ALP activity was measured in the culture media (data not shown).

Discussion

The overall objective of this study was to explore how dynamic compression (DC) would influence the functional development of cartilaginous grafts engineered using different sources of stem cells. In agreement with previous studies (Huang et al., 2010, Bian et al., 2012, Thorpe et al., 2013, Mauck et al., 2007, Kisiday et al., 2009), we showed the application of DC can be beneficial to the development of cartilaginous grafts engineered using BMSCs, with loading having the potential to increase matrix accumulation and the mechanical properties of the graft while simultaneously suppressing collagen type I accumulation and mineral deposition. In contrast, DC did not have a dramatic effect on the functional development of cartilaginous grafts engineered using FPSCs, with no significant changes observed in matrix synthesis or mechanical properties of engineered tissues subjected to loading.

Stem cells isolated from both BM and FP tissue generated cartilaginous constructs with a proteoglycan content, measured as a percentage of wet weight, approaching that observed in the skeletally immature tissue (Gannon et al., 2012). This in turn led to the development of tissues with mechanical properties of a similar order of magnitude to native skeletally immature tissue, with the equilibrium modulus reaching up to 300kPa (see Fig. 2 and Supplementary Fig. 2). Perhaps the most striking difference between the tissues engineered using BM and FP derived stem cells was the spatial accumulation of matrix within the hydrogel. Greater levels of extracellular matrix (ECM) accumulation were observed around the periphery of FP constructs from both donors, while a more homogenous distribution of ECM was observed in BM constructs (see Fig. 1B and Supplementary Fig. 1B). This may be due to the fact that FPSCs were more metabolically active than BMSCs, leading to the development of nutrient deprived regions towards the center of the FP constructs. The greater levels of proliferation observed in FP constructs (Fig. 1A) may also be contributing to the development of such a nutrient deprived core region in the engineered tissue. Alternatively, it may be possible that nutrient deprived regions

develop in the center of both FP and BM constructs, but that BMSCs are better equipped to thrive in such conditions than FPSCs. Evidence against this hypothesis can be found in recent studies which demonstrate that BMSCs are sensitive to nutrient supply and undergo superior chondrogenesis under optimal nutrient conditions (Farrell et al., 2012), although direct comparisons of different stem cell types in nutrient deprived conditions have yet to be undertaken. Further studies are required to compare the metabolic requirements of different sources of stem cells, as if differences do exist then the culture conditions required to engineer functional cartilage grafts will need to be optimized for specific stem cell types.

Dynamic compression did not appear to enhance the development of cartilage grafts engineered using FPSCs. This may be due to the fact that these cells possess a strong intrinsic potential to generate a matrix rich in proteoglycans following TGF-β3 stimulation (generating tissues with a sGAG content approaching that of native skeletal immature articular cartilage), and hence chondrogenesis of FPSCs is not further enhanced following the application of DC. Furthermore, when DC was observed to increase ECM synthesis in BM constructs, these changes were relatively small. As previous studies provide support for the hypothesis that mechanical load promotes chondrogenesis of human mesenchymal stem cells through the TGF-β pathway by up-regulating TGF-β gene expression and protein synthesis (Li et al., 2010a), it is perhaps unsurprising that dynamic compression has only a small effect on ECM synthesis in culture environment containing abundant TGF-β3. Further work is required to identify if alternative loading periods or magnitudes would have a more positive impact on chondrogenesis of FP derived stem cells.

The spatial differences in ECM accumulation observed in BM and FP constructs (and indeed between stem cells taken from the same tissue source but from different donors) may provide an alternative explanation for why DC did not consistently result in an increase in matrix synthesis. Finite element models have demonstrated that localization of ECM to the outer layer of the engineered tissue, similar to that

observed in FP constructs from both donors, can result in an order of magnitude change in the peak volumetric strain and deviatoric strain in the tissue, and to reduce the peak pore pressure in the centre of the construct (Khoshgoftar et al., 2013). Therefore the spatial mechanical environment within the FP and BM grafts are likely very different, even though the same global deformation is being applied to each engineered tissue. It is therefore possible that the more homogenous ECM distribution observed in the BMSCs seeded construct is leading to the development of a more chondrogenic mechanical environment (at least in parts of the construct) when these tissues are subjected to DC. Similarly, donor to donor variability in the response of BMSCs to loading may also potentially be explained by variations in ECM accumulation. The fact that BMSCs from donor 1 responded anabolically to the application of DC, while donor 2 did not, may also be due to the greater levels of ECM accumulation observed in the grafts generated from donor 2 (sGAG accumulation was approximately two fold higher for donor 2; see Fig. 1A and Supplementary Fig. 1A). Such differences may necessitate alterations to the magnitude of global deformation applied to a given engineered tissue as it develops to create a pro-chondrogenic mechanical environment at the cellular level (Khoshgoftar et al., 2013). These results also serve to highlight the challenges of further exploring donor dependent variability in the response of stem cells to biophysical cues, which is beyond the scope of the present study. Given that spatial ECM accumulation determines the local cellular mechanical environment in engineered tissues subjected to DC, and that ECM develops uniquely with the engineered tissue of each donor, it is difficult if not impossible to attribute differences in matrix synthesis in response to DC between the different donors to either donor dependent stem cell mechano-responsiveness, differences in ECM accumulation between donors or a combination of both.

It was found that a small, but significant, increase in sGAG and collagen accumulation (~8% increase in sGAG and collagen accumulation with the application of DC) led to a relatively higher increase (~25%) in the equilibrium modulus of the

BM constructs (Fig. 2). Previous studies have found that the delayed application of dynamic compression to cartilaginous tissues engineered using BMSCs can lead to improvements in the mechanical properties of the grafts without significantly changing the bulk levels of sGAG and collagen accumulation within the tissue (Huang et al., 2010). DC did however lead to an altered distribution of matrix components within the engineered tissue, which may in turn contribute to the improved apparent mechanical properties (Huang et al., 2010). While such dramatic changes in ECM distribution were not observed in this study, which may be due to the fact that we only applied 1 hour of DC compared to 4 hours used in other studies, subtle changes in pericellular sGAG accumulation were observed following the application of loading. Any loading regime that leads to the development of a more homogenous engineered tissue should lead to an increase in the apparent mechanical properties independent of any increase in biochemical composition (Khoshgoftar et al., 2012).

In agreement with a number of recent studies (Thorpe et al., 2012, Bian et al., 2012, Vinardell et al., 2012a, Steward et al., 2012), we also found that mechanical cues would appear to be critical to the maintenance of the cartilage phenotype in chondrogenically primed BMSCs. Collagen type I accumulation and mineralization within BM constructs was suppressed by the application of DC. This suggests that much of the concern associated with hypertrophy and endochondral ossification of chondrogenically primed BMSCs could be associated with the absence of mechanical cues within most *in vitro* culture conditions and many *in vivo* models (such as subcutaneous implantation) used to access the phenotypic stability of tissue engineered grafts. Under the appropriate mechanical environment within load bearing cartilage defects, it may be that BMSCs will generate phenotypically stable articular cartilage (Steck et al., 2009). In contrast, cartilage constructs engineered using FPSCs did not exhibit any mineralization. This is in line with other findings that FPSCs have a lower tendency to proceed endochondral pathway compared to BMSCs (Vinardell et al., 2012b).

In conclusion, both BM and FP derived stem cells were capable of generating cartilaginous tissues with near native levels of sGAG content and mechanical properties approaching that observed in skeletally immature animals. Collagen accumulation, as has been observed in numerous cartilage tissue engineering studies, was still significantly lower than the native tissue. The application of dynamic compression could at best lead to small increases in ECM accumulation, although not for all donors or cell types. Based on the results of this study, it is difficult to argue that such small increases in ECM synthesis would warrant the use of bioreactors in a clinical context for cartilage regeneration. Whether the potential increases in mechanical properties of the graft, or the suppression of hypertrophy, merits their use requires further *in vivo* studies.

Acknowledgements

Funding was provided by the European Research Council Starter Grant (StemRepair – Project number 258463) and a SFI President of Ireland Young Researcher Award (08/Y15/B1336).

References

BIAN, L., ZHAI, D. Y., TOUS, E., RAI, R., MAUCK, R. L. & BURDICK, J. A. 2011. Enhanced MSC chondrogenesis following delivery of TGF-β3 from alginate microspheres within hyaluronic acid hydrogels in vitro and in vivo. *Biomaterials,* 32**,** 6425-6434.

BIAN, L., ZHAI, D. Y., ZHANG, E. C., MAUCK, R. L. & BURDICK, J. A. 2012. Dynamic compressive loading enhances cartilage matrix synthesis and distribution and suppresses hypertrophy in hMSC-laden hyaluronic acid hydrogels. *Tissue Eng Part A,* 18**,** 715-24.

BUCKLEY, C. T. & KELLY, D. J. 2012. Expansion in the presence of FGF-2 enhances the functional development of cartilaginous tissues engineered using infrapatellar fat pad derived MSCs. *J Mech Behav Biomed Mater,* 11**,** 102-11.

BUCKLEY, C. T., THORPE, S. D., O'BRIEN, F. J., ROBINSON, A. J. & KELLY, D. J. 2009. The effect of concentration, thermal history and cell seeding density on the initial mechanical properties of agarose hydrogels. *J Mech Behav Biomed Mater,* 2**,** 512-21.

BUCKLEY, C. T., VINARDELL, T. & KELLY, D. J. 2010a. Oxygen tension differentially regulates the functional properties of cartilaginous tissues engineered from infrapatellar fat pad derived MSCs and articular chondrocytes. *Osteoarthritis Cartilage,* 18**,** 1345-54.

BUCKLEY, C. T., VINARDELL, T., THORPE, S. D., HAUGH, M. G., JONES, E., MCGONAGLE, D. & KELLY, D. J. 2010b. Functional properties of cartilaginous tissues engineered from infrapatellar fat pad-derived mesenchymal stem cells. *J Biomech,* 43**,** 920-6.

BUSCHMANN, M. D., GLUZBAND, Y. A., GRODZINSKY, A. J. & HUNZIKER, E. B. 1995. Mechanical compression modulates matrix biosynthesis in chondrocyte/agarose culture. *J Cell Sci,* 108 (Pt 4)**,** 1497-508.

DEMARTEAU, O., WENDT, D., BRACCINI, A., JAKOB, M., SCHAFER, D., HEBERER, M. & MARTIN, I. 2003. Dynamic compression of cartilage constructs engineered from expanded human articular chondrocytes. *Biochem Biophys Res Commun,* 310**,** 580-8.

DRAGOO, J. L., SAMIMI, B., ZHU, M., HAME, S. L., THOMAS, B. J., LIEBERMAN, J. R., HEDRICK, M. H. & BENHAIM, P. 2003. Tissue-engineered cartilage and bone using stem cells from human infrapatellar fat pads. *J Bone Joint Surg Br,* 85**,** 740-7.

ENGLISH, A., JONES, E. A., CORSCADDEN, D., HENSHAW, K., CHAPMAN, T., EMERY, P. & MCGONAGLE, D. 2007. A comparative assessment of cartilage and joint fat pad as a potential source of cells for autologous therapy development in knee osteoarthritis. *Rheumatology (Oxford),* 46**,** 1676-83.

ERICKSON, G. R., GIMBLE, J. M., FRANKLIN, D. M., RICE, H. E., AWAD, H. & GUILAK, F. 2002. Chondrogenic potential of adipose tissue-derived stromal cells in vitro and in vivo. *Biochem Biophys Res Commun,* 290**,** 763-9.

ERICKSON, I. E., HUANG, A. H., CHUNG, C., LI, R. T., BURDICK, J. A. & MAUCK, R. L. 2009. Differential maturation and structure-function relationships in mesenchymal stem cell- and chondrocyte-seeded hydrogels. *Tissue Eng Part A,* 15**,** 1041-52.

FARRELL, M. J., COMEAU, E. S. & MAUCK, R. L. 2012. Mesenchymal stem cells produce functional cartilage matrix in three-dimensional culture in regions of optimal nutrient supply. *Eur Cell Mater,* 23**,** 425-40.

FELIMBAN, R., YE, K., TRAIANEDES, K., DI BELLA, C., CROOK, J., WALLACE, G. G., QUIGLEY, A., CHOONG,

P. F. M. & MYERS, D. E. 2014. Differentiation of stem cells from human infrapatellar fat pad: Characterization of cells undergoing chondrogenesis. *Tissue Engineering - Part A,* 20**,** 2213-2223.

GANNON, A. R., NAGEL, T. & KELLY, D. J. 2012. The role of the superficial region in determining the dynamic properties of articular cartilage. *Osteoarthritis Cartilage,* 20**,** 1417-25.

GIMBLE, J. M. & GUILAK, F. 2003. Adipose-derived adult stem cells: isolation, characterization, and differentiation potential. *Cytotherapy,* 5**,** 362-369.

GUILAK, F., AWAD, H. A., FERMOR, B., LEDDY, H. A. & GIMBLE, J. M. 2004. Adipose-derived adult stem cells for cartilage tissue engineering. *Biorheology,* 41**,** 389-99.

HAUGH, M. G., MEYER, E. G., THORPE, S. D., VINARDELL, T., DUFFY, G. P. & KELLY, D. J. 2011. Temporal and spatial changes in cartilage-matrix-specific gene expression in mesenchymal stem cells in response to dynamic compression. *Tissue Eng Part A,* 17**,** 3085-93.

HUANG, A. H., FARRELL, M. J., KIM, M. & MAUCK, R. L. 2010. Long-term dynamic loading improves the mechanical properties of chondrogenic mesenchymal stem cell-laden hydrogel. *Eur Cell Mater,* 19**,** 72-85.

HUANG, C. Y., REUBEN, P. M. & CHEUNG, H. S. 2005. Temporal expression patterns and corresponding protein inductions of early responsive genes in rabbit bone marrow-derived mesenchymal stem cells under cyclic compressive loading. *Stem Cells,* 23**,** 1113-21.

IGNAT'EVA, N. Y., DANILOV, N. A., AVERKIEV, S. V., OBREZKOVA, M. V., LUNIN, V. V. & SOBOL', E. N. 2007. Determination of hydroxyproline in tissues and the evaluation of the collagen content of the tissues. *Journal of Analytical Chemistry,* 62**,** 51-57.

JOHNSTONE, B., HERING, T. M., CAPLAN, A. I., GOLDBERG, V. M. & YOO, J. U. 1998. In vitro chondrogenesis of bone marrow-derived mesenchymal progenitor cells. *Exp Cell Res,* 238**,** 265-72.

JURGENS, W. J. F. M., VAN DIJK, A., DOULABI, B. Z., NIESSEN, F. B., RITT, M. J. P. F., VAN MILLIGEN, F. J. & HELDER, M. N. 2009. Freshly isolated stromal cells from the infrapatellar fat pad are suitable for a one-step surgical procedure to regenerate cartilage tissue. *Cytotherapy,* 11**,** 1052-1064.

KAFIENAH, W., MISTRY, S., DICKINSON, S. C., SIMS, T. J., LEARMONTH, I. & HOLLANDER, A. P. 2007. Three-dimensional cartilage tissue engineering using adult stem cells from osteoarthritis patients. *Arthritis Rheum,* 56**,** 177-87.

KAFIENAH, W. & SIMS, T. J. 2004. Biochemical methods for the analysis of tissue-engineered cartilage. *Methods Mol Biol,* 238**,** 217-30.

KELLY, D. J. & JACOBS, C. R. 2010. The role of mechanical signals in regulating chondrogenesis and osteogenesis of mesenchymal stem cells. *Birth Defects Res C Embryo Today,* 90**,** 75-85.

KHOSHGOFTAR, M., WILSON, W., ITO, K. & VAN DONKELAAR, C. C. 2012. Influence of tissue- and cell-scale extracellular matrix distribution on the mechanical properties of tissue-engineered cartilage. *Biomech Model Mechanobiol*.

KHOSHGOFTAR, M., WILSON, W., ITO, K. & VAN DONKELAAR, R. 2013. The effects of matrix inhomogeneities on the cellular mechanical environment in tissue-engineered cartilage: an in silico investigation. *Tissue Eng Part C Methods*.

KIM, Y. J., SAH, R. L., DOONG, J. Y. & GRODZINSKY, A. J. 1988. Fluorometric assay of DNA in cartilage explants using Hoechst 33258. *Anal Biochem,* 174**,** 168-76.

KISIDAY, J. D., FRISBIE, D. D., MCILWRAITH, C. W. & GRODZINSKY, A. J. 2009. Dynamic compression

stimulates proteoglycan synthesis by mesenchymal stem cells in the absence of chondrogenic cytokines. *Tissue Eng Part A,* 15**,** 2817-24.

LENNON, D. P. & CAPLAN, A. I. 2006. Isolation of human marrow-derived mesenchymal stem cells. *Exp Hematol,* 34**,** 1604-5.

LI, J., ZHAO, Z., YANG, J., LIU, J., WANG, J., LI, X. & LIU, Y. 2009. p38 MAPK mediated in compressive stress-induced chondrogenesis of rat bone marrow MSCs in 3D alginate scaffolds. *J Cell Physiol,* 221**,** 609-17.

LI, Z., KUPCSIK, L., YAO, S. J., ALINI, M. & STODDART, M. J. 2010a. Mechanical load modulates chondrogenesis of human mesenchymal stem cells through the TGF-beta pathway. *J Cell Mol Med,* 14**,** 1338-46.

LI, Z., YAO, S. J., ALINI, M. & STODDART, M. J. 2010b. Chondrogenesis of human bone marrow mesenchymal stem cells in fibrin-polyurethane composites is modulated by frequency and amplitude of dynamic compression and shear stress. *Tissue Eng Part A,* 16**,** 575-84.

LIU, Y., BUCKLEY, C. T., DOWNEY, R., MULHALL, K. J. & KELLY, D. J. 2012. The role of environmental factors in regulating the development of cartilaginous grafts engineered using osteoarthritic human infrapatellar fat pad-derived stem cells. *Tissue Eng Part A,* 18**,** 1531-41.

LIU, Y., BUCKLEY, C. T., MULHALL, K. J. & KELLY, D. J. 2013. Combining BMP-6, TGF-β3 and hydrostatic pressure stimulation enhances the functional development of cartilage tissues engineered using human infrapatellar fat pad derived stem cells. *Biomaterials Science,* 1**,** 745.

MATSIKO, A., LEVINGSTONE, T. J., O'BRIEN, F. J. & GLEESON, J. P. 2012. Addition of hyaluronic acid improves cellular infiltration and promotes early-stage chondrogenesis in a collagen-based scaffold for cartilage tissue engineering. *Journal of the Mechanical Behavior of Biomedical Materials,* 11**,** 41-52.

MAUCK, R. L., BYERS, B. A., YUAN, X. & TUAN, R. S. 2007. Regulation of cartilaginous ECM gene transcription by chondrocytes and MSCs in 3D culture in response to dynamic loading. *Biomech Model Mechanobiol,* 6**,** 113-25.

MAUCK, R. L., SOLTZ, M. A., WANG, C. C., WONG, D. D., CHAO, P. H., VALHMU, W. B., HUNG, C. T. & ATESHIAN, G. A. 2000. Functional tissue engineering of articular cartilage through dynamic loading of chondrocyte-seeded agarose gels. *J Biomech Eng,* 122**,** 252-60.

MAUCK, R. L., YUAN, X. & TUAN, R. S. 2006. Chondrogenic differentiation and functional maturation of bovine mesenchymal stem cells in long-term agarose culture. *Osteoarthritis Cartilage,* 14**,** 179-89.

MIKIC, B., ISENSTEIN, A. L. & CHHABRA, A. 2004. Mechanical modulation of cartilage structure and function during embryogenesis in the chick. *Ann Biomed Eng,* 32**,** 18-25.

MIKIC, B., JOHNSON, T. L., CHHABRA, A. B., SCHALET, B. J., WONG, M. & HUNZIKER, E. B. 2000. Differential effects of embryonic immobilization on the development of fibrocartilaginous skeletal elements. *J Rehabil Res Dev,* 37**,** 127-33.

MOW, V. C. & WANG, C. C. 1999. Some bioengineering considerations for tissue engineering of articular cartilage. *Clin Orthop Relat Res***,** S204-23.

PEI, M., HE, F., BOYCE, B. M. & KISH, V. L. 2009. Repair of full-thickness femoral condyle cartilage defects using allogeneic synovial cell-engineered tissue constructs. *Osteoarthritis Cartilage,* 17**,** 714-22.

PEI, M., HE, F. & VUNJAK-NOVAKOVIC, G. 2008. Synovium-derived stem cell-based chondrogenesis. *Differentiation,* 76**,** 1044-56.

PELTTARI, K., WINTER, A., STECK, E., GOETZKE, K., HENNIG, T., OCHS, B. G., AIGNER, T. & RICHTER, W. 2006. Premature induction of hypertrophy during in vitro chondrogenesis of human mesenchymal stem cells correlates with calcification and vascular invasion after ectopic transplantation in SCID mice. *Arthritis Rheum,* 54**,** 3254-66.

PITTENGER, M. F., MACKAY, A. M., BECK, S. C., JAISWAL, R. K., DOUGLAS, R., MOSCA, J. D., MOORMAN, M. A., SIMONETTI, D. W., CRAIG, S. & MARSHAK, D. R. 1999. Multilineage potential of adult human mesenchymal stem cells. *Science,* 284**,** 143-7.

RIEPPO, J., HYTTINEN, M., HALMESMAKI, E., RUOTSALAINEN, H., VASARA, A., KIVIRANTA, I., JURVELIN, J. & HELMINEN, H. 2009. Changes in spatial collagen content and collagen network architecture in porcine articular cartilage during growth and maturation. *Osteoarthritis and Cartilage,* 17**,** 448-455.

SHEEHY, E. J., BUCKLEY, C. T. & KELLY, D. J. 2012. Oxygen tension regulates the osteogenic, chondrogenic and endochondral phenotype of bone marrow derived mesenchymal stem cells. *Biochem Biophys Res Commun,* 417**,** 305-10.

STECK, E., FISCHER, J., LORENZ, H., GOTTERBARM, T., JUNG, M. & RICHTER, W. 2009. Mesenchymal stem cell differentiation in an experimental cartilage defect: restriction of hypertrophy to bone-close neocartilage. *Stem Cells Dev,* 18**,** 969-78.

STEWARD, A. J., THORPE, S. D., VINARDELL, T., BUCKLEY, C. T., WAGNER, D. R. & KELLY, D. J. 2012. Cell-matrix interactions regulate mesenchymal stem cell response to hydrostatic pressure. *Acta Biomater,* 8**,** 2153-9.

THORPE, S. D., BUCKLEY, C. T., STEWARD, A. J. & KELLY, D. J. 2012. European Society of Biomechanics S.M. Perren Award 2012: the external mechanical environment can override the influence of local substrate in determining stem cell fate. *J Biomech,* 45**,** 2483-92.

THORPE, S. D., BUCKLEY, C. T., VINARDELL, T., O'BRIEN, F. J., CAMPBELL, V. A. & KELLY, D. J. 2008. Dynamic compression can inhibit chondrogenesis of mesenchymal stem cells. *Biochem Biophys Res Commun,* 377**,** 458-62.

THORPE, S. D., BUCKLEY, C. T., VINARDELL, T., O'BRIEN, F. J., CAMPBELL, V. A. & KELLY, D. J. 2010. The response of bone marrow-derived mesenchymal stem cells to dynamic compression following TGF-beta3 induced chondrogenic differentiation. *Ann Biomed Eng,* 38**,** 2896-909.

THORPE, S. D., NAGEL, T., CARROLL, S. F. & KELLY, D. J. 2013. Modulating gradients in regulatory signals within mesenchymal stem cell seeded hydrogels: a novel strategy to engineer zonal articular cartilage. *PLoS One,* 8**,** e60764.

VINARDELL, T., BUCKLEY, C. T., THORPE, S. D. & KELLY, D. J. 2011. Composition-function relations of cartilaginous tissues engineered from chondrocytes and mesenchymal stem cells isolated from bone marrow and infrapatellar fat pad. *J Tissue Eng Regen Med,* 5**,** 673-683.

VINARDELL, T., ROLFE, R. A., BUCKLEY, C. T., MEYER, E. G., AHEARNE, M., MURPHY, P. & KELLY, D. J. 2012a. Hydrostatic pressure acts to stabilise a chondrogenic phenotype in porcine joint tissue derived stem cells. *Eur Cell Mater,* 23**,** 121-32; discussion 133-4.

VINARDELL, T., SHEEHY, E. J., BUCKLEY, C. T. & KELLY, D. J. 2012b. A comparison of the functionality and in vivo phenotypic stability of cartilaginous tissues engineered from different stem cell sources. *Tissue Eng Part A,* 18**,** 1161-70.

WAKITANI, S., GOTO, T., PINEDA, S. J., YOUNG, R. G., MANSOUR, J. M., CAPLAN, A. I. & GOLDBERG, V. M. 1994. Mesenchymal cell-based repair of large, full-thickness defects of articular cartilage. *J Bone Joint Surg Am,* 76**,** 579-92.

WICKHAM, M. Q., ERICKSON, G. R., GIMBLE, J. M., VAIL, T. P. & GUILAK, F. 2003. Multipotent Stromal Cells Derived From the Infrapatellar Fat Pad of the Knee. *Clinical Orthopaedics and Related Research,* 412**,** 196-212 10.1097/01.blo.0000072467.53786.ca.

WISE, J. K., YARIN, A. L., MEGARIDIS, C. M. & CHO, M. 2009. Chondrogenic differentiation of human mesenchymal stem cells on oriented nanofibrous scaffolds: engineering the superficial zone of articular cartilage. *Tissue Eng Part A,* 15**,** 913-21.

YE, K., FELIMBAN, R., TRAIANEDES, K., MOULTON, S. E., WALLACE, G. G., CHUNG, J., QUIGLEY, A., CHOONG, P. F. M. & MYERS, D. E. 2014. Chondrogenesis of infrapatellar fat pad derived adipose stem cells in 3D printed chitosan scaffold. *PLoS ONE,* 9.

YOO, J. U., BARTHEL, T. S., NISHIMURA, K., SOLCHAGA, L., CAPLAN, A. I., GOLDBERG, V. M. & JOHNSTONE, B. 1998. The chondrogenic potential of human bone-marrow-derived mesenchymal progenitor cells. *J Bone Joint Surg Am,* 80**,** 1745-57.

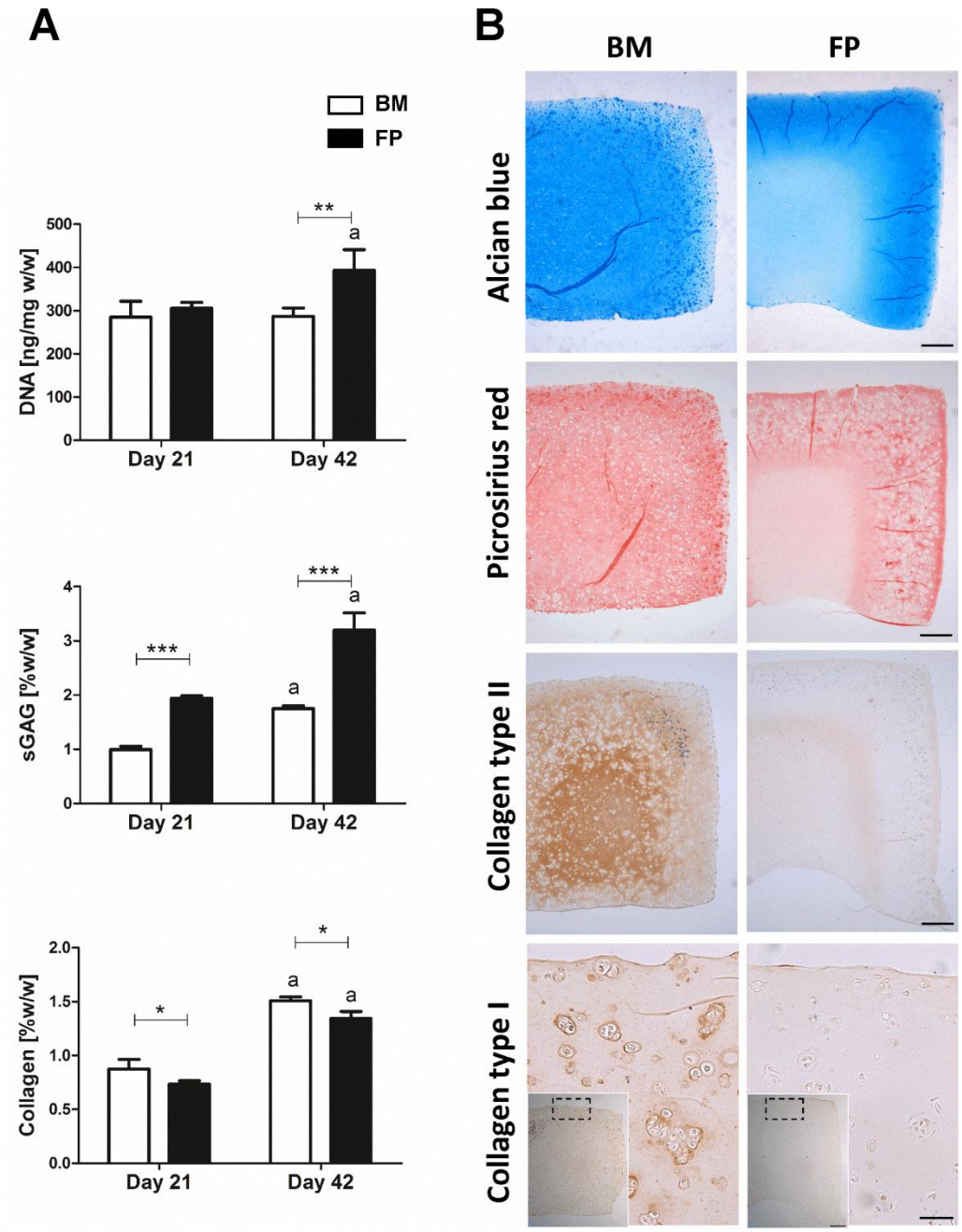

Figure 1. Temporal and spatial development of free swelling (FS) cultured BM and FP constructs. (A) DNA (ng/mg w/w), sGAG (%w/w) and collagen (%w/w) content of FS cultured BM and FP constructs at day 21 and 42; a: $p<0.05$ vs. same construct type at day 21; *: $p<0.05$, **: $p<0.01$; ***: $p<0.001$. (B) Alcian blue, picrosirius red, collagen type II and I staining of FS cultured BM and FP constructs at day 42. Scale bar in alcian blue, picrosirius red and collagen type II staining: 500 µm. Scale bar in collagen type I staining: 50 µm. Inserted images were taken at a low magnification to show staining at a bulk construct level, with box regions indicating area from where high magnification images were taken. Scale bar in inserted image: 500 µm.

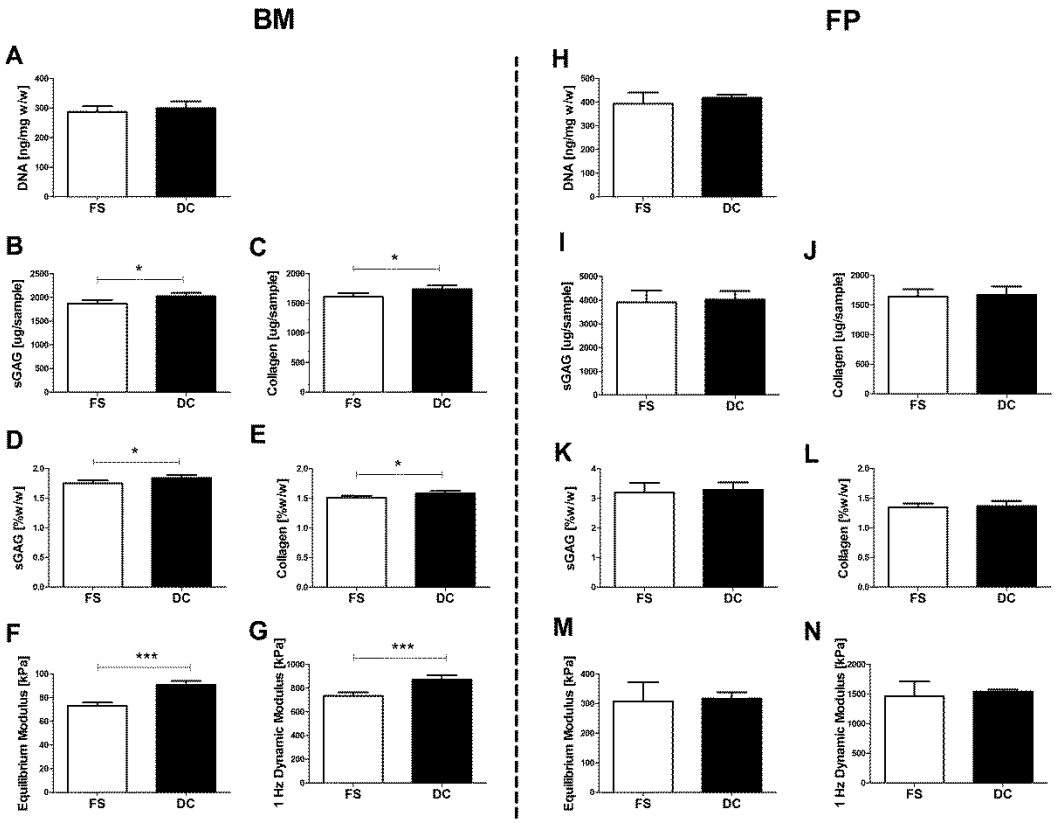

Figure 2. Biochemical content and mechanical properties of BM and FP constructs in free swelling (FS) and dynamic compression (DC) culture at day 42. (A, H) DNA content (ng/mg w/w); (B, I) sGAG content (µg/sample); (C, J) Collagen content (µg/sample); (D, K) sGAG content (% w/w); (E, L) Collagen content (% w/w); (F, M) Equilibrium modulus (kPa); (G, N) 1Hz dynamic modulus (kPa). *: $p<0.05$, ***: $p<0.001$.

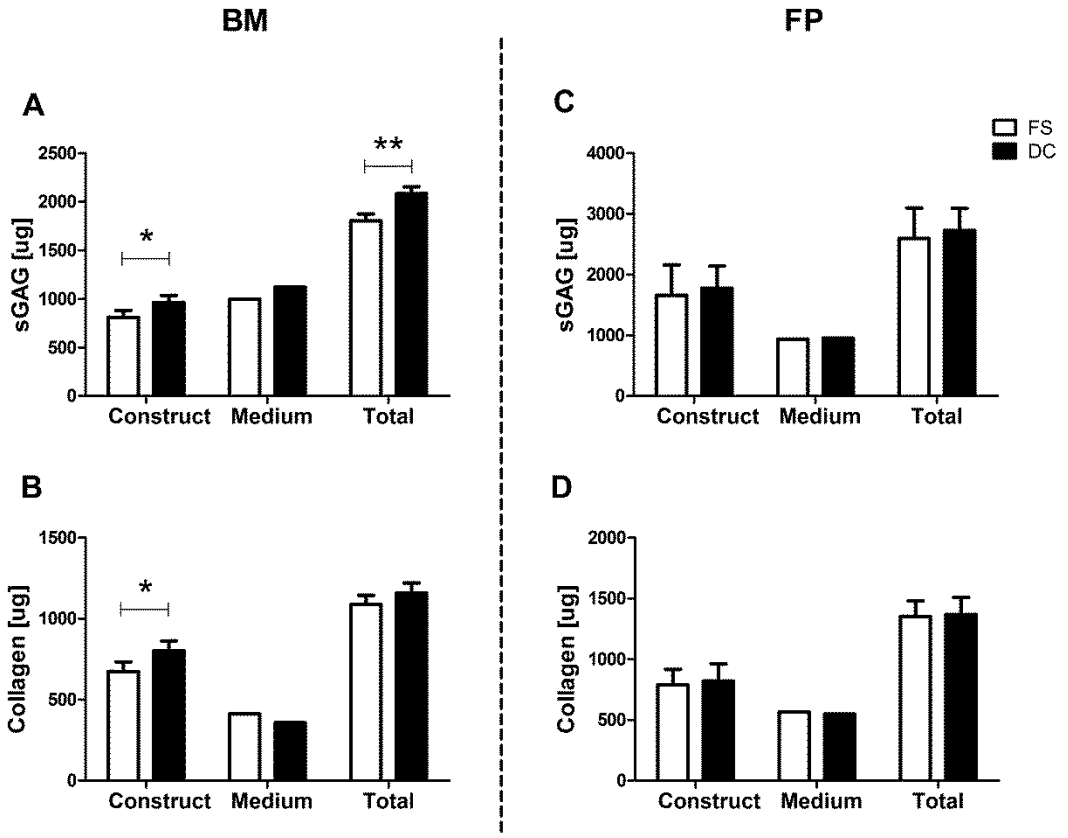

Figure 3. sGAG and collagen content accumulated within the constructs, released into media and the total synthesized (accumulated + released) from day 21 to day 42 in BM and FP constructs in FS and DC culture. (A, C) sGAG content (μg); (B, D) collagen content (μg). Media samples from day 21 to day 42 were analysed for sGAG or collagen content released from the constructs (n=1 per group, as media from each individual construct were pooled). sGAG or collagen content accumulated within constructs from day 21 to day 42 were calculated by subtracting the mean value of sGAG or collagen content of day 21 samples from the value of sGAG or collagen content of each individual day 42 samples (n=4 per group). Total amount of sGAG or collagen synthesis from day 21 to day 42 was calculated by summing up the amount accumulated within constructs and the amount released into media. *: $p<0.05$; **: $p<0.01$.

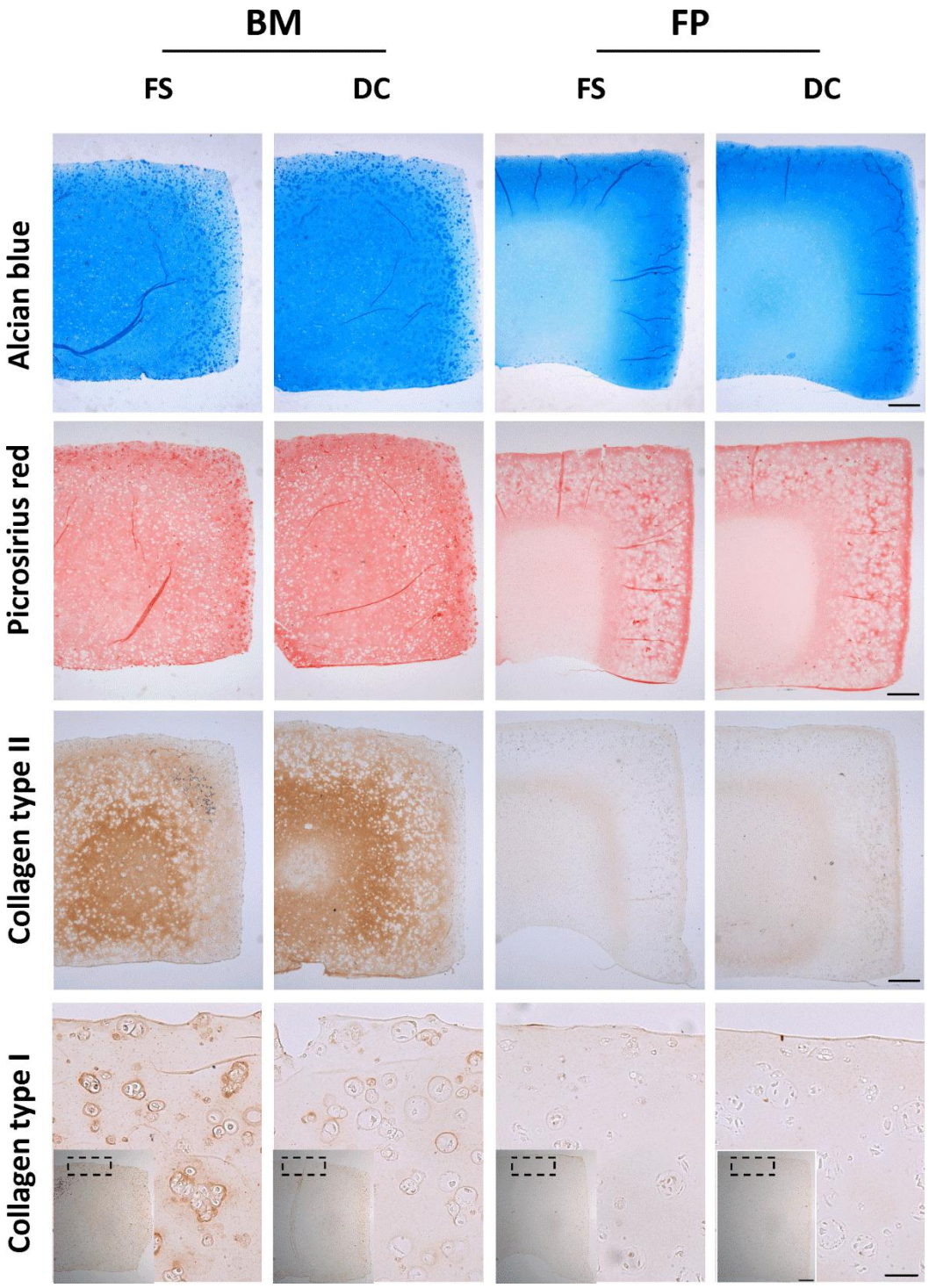

Figure 4. Histological and immunohistological staining of BM and FP constructs in FS and DC culture at day 42. Scale bar in alcian blue, picrosirius red and collagen type II staining: 500 µm. Scale bar in collagen type I staining: 50 µm. Inserted images were taken at a low magnification to show staining at a bulk construct level, with box regions indicating area from where high magnification images were taken. Scale bar in inserted image: 500 µm.

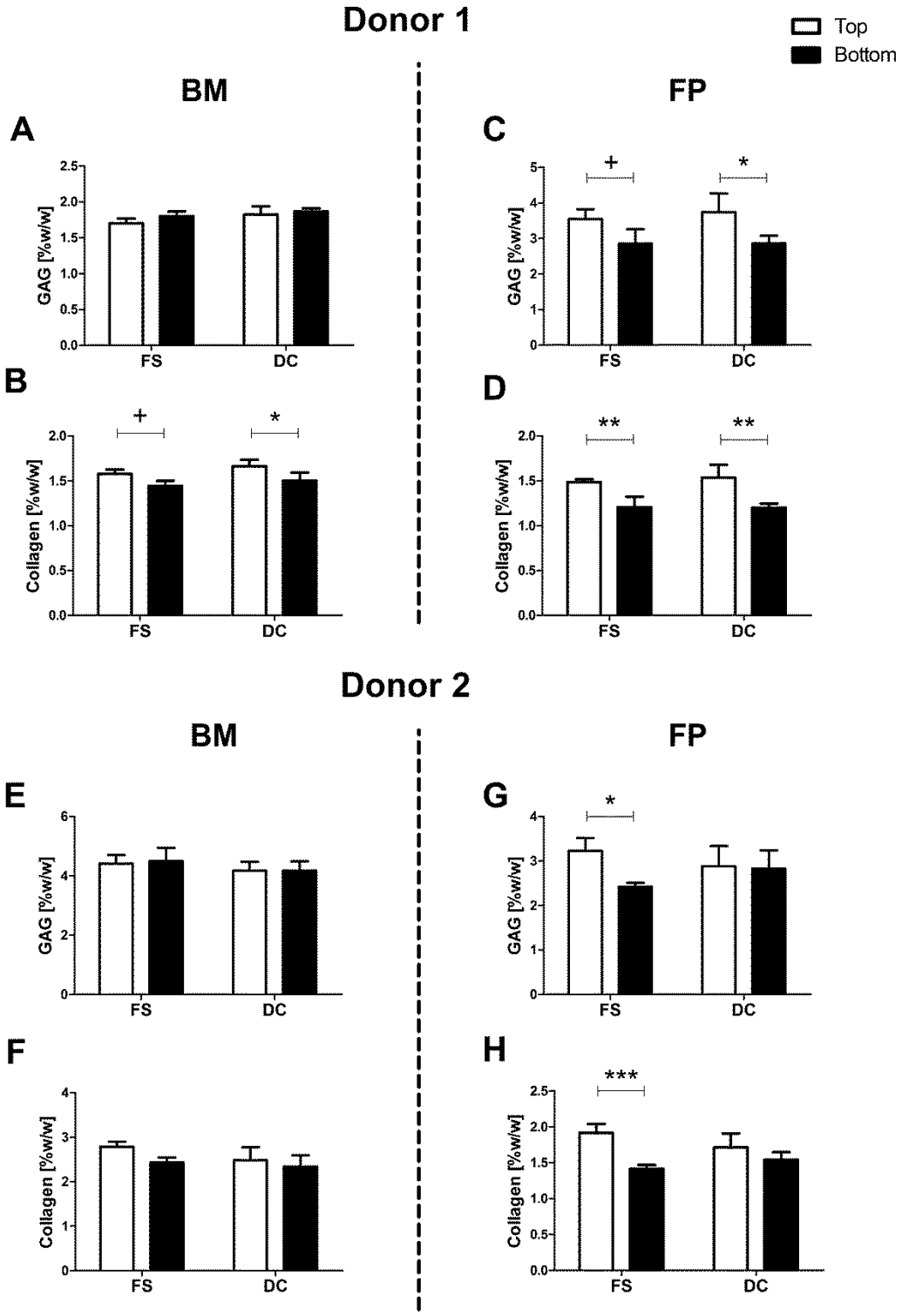

Figure 5. Biochemical content of top and bottom halves of BM and FP constructs, engineered using both donors, in FS and DC culture at day 42. (A, C, E, G) sGAG content (%w/w); (B, D, F, H) collagen content (%w/w). +: $p<0.1$; *: $p<0.05$, **: $p<0.01$; ***: $p<0.001$.

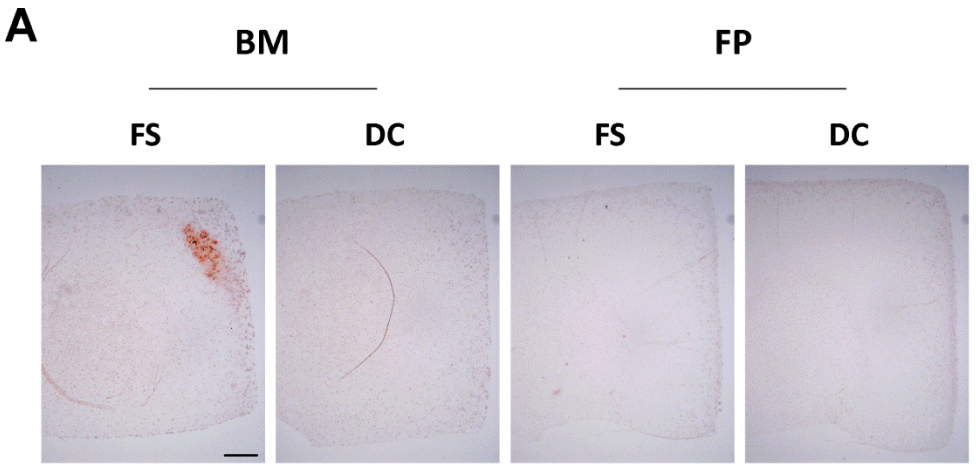

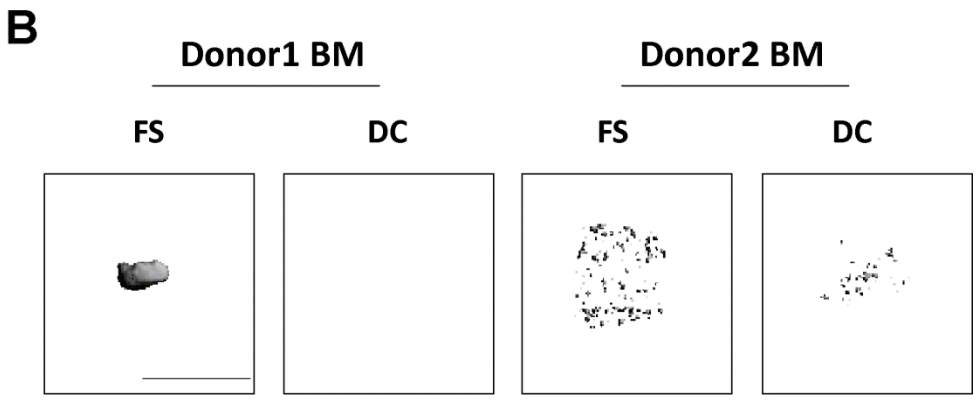

C

	FS (mineral volume mm^3)	DC (mineral volume mm^3)
Donor 1 BM	0.1859	0
	0	0
Donor 2 BM	0.0285	0.0014
	0.0073	0.0006
Mean ± SD	0.0554 ± 0.0878	0.0005 ± 0.0007

Figure 6. Assessment of mineralization in BM and FP constructs, engineered using both donors, in FS and DC culture at day 42. (A) Representative alizarin red staining of mineral deposition in BM and FP constructs in FS and DC culture at day 42; scale bar: 500 µm. (B) 3D images obtained with µCT scanning of mineral deposition within BM constructs in FS and DC culture. Scale bar: 1mm. (C) Volume of minerals within BM constructs in FS and DC culture. Two constructs per group were scanned using µCT.

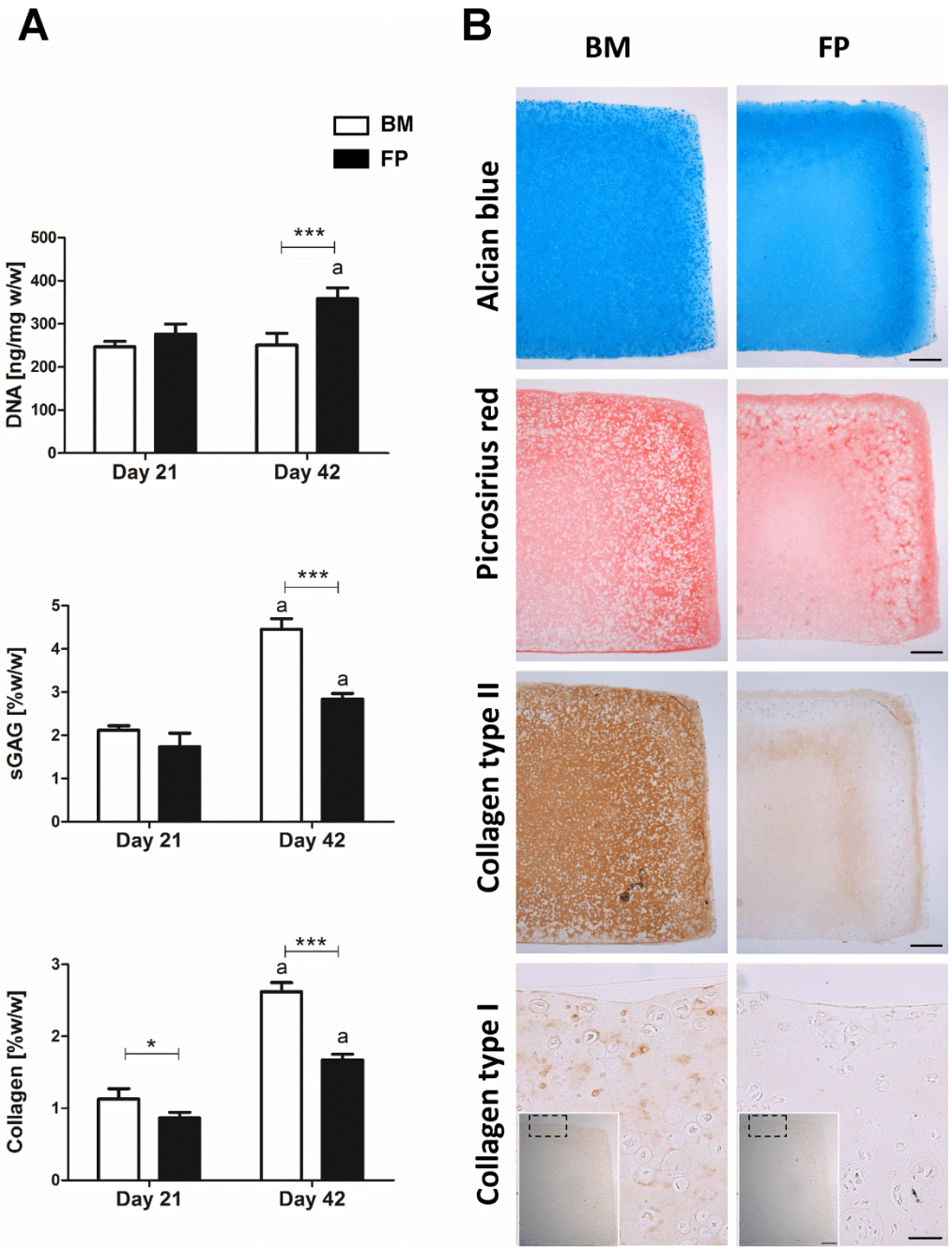

Supplementary Figure 1. Temporal and spatial development of free swelling (FS) cultured BM and FP constructs engineered using donor 2. (A) DNA (ng/mg w/w), sGAG (%w/w) and collagen (%w/w) content of FS cultured BM and FP constructs from donor 2 at day 21 and 42; a: $p<0.05$ vs. same construct type at day 21; *: $p<0.05$, **: $p<0.01$; ***: $p<0.001$. (B) Alcian blue, picrosirius red, collagen type II and I staining of FS cultured BM and FP constructs from donor 2 at day 42. Scale bar in alcian blue, picrosirius red and collagen type II staining: 500 µm. Scale bar in collagen type I staining: 50 µm. Inserted images were taken at a low magnification to show staining at a bulk construct level, with box regions indicating area from where high magnification images were taken. Scale bar in inserted image: 500 µm.

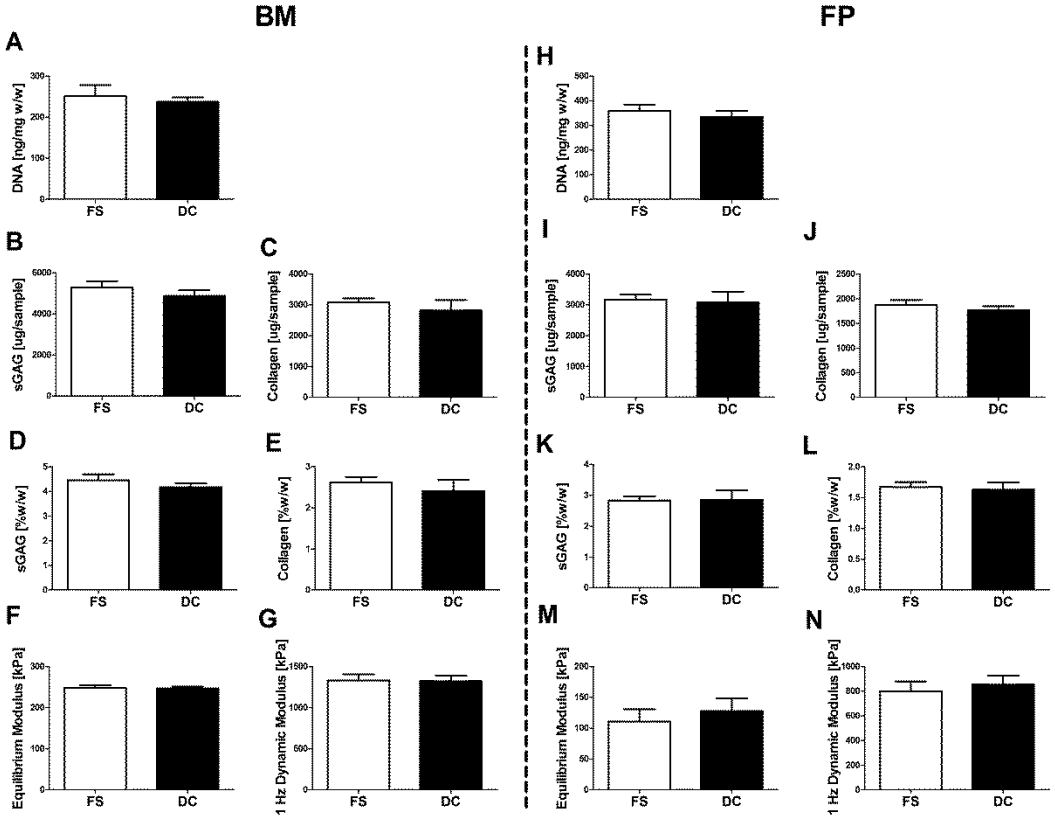

Supplementary Figure 2. Biochemical content and mechanical properties of BM and FP constructs, engineered using donor 2, in FS and DC culture at day 42. (A, H) DNA content (ng/mg w/w); (B, I) sGAG content (μg/sample); (C, J) Collagen content (μg/sample); (D, K) sGAG content (% w/w); (E, L) Collagen content (% w/w); (F, M) Equilibrium modulus (kPa); (G, N) 1Hz dynamic modulus (kPa).

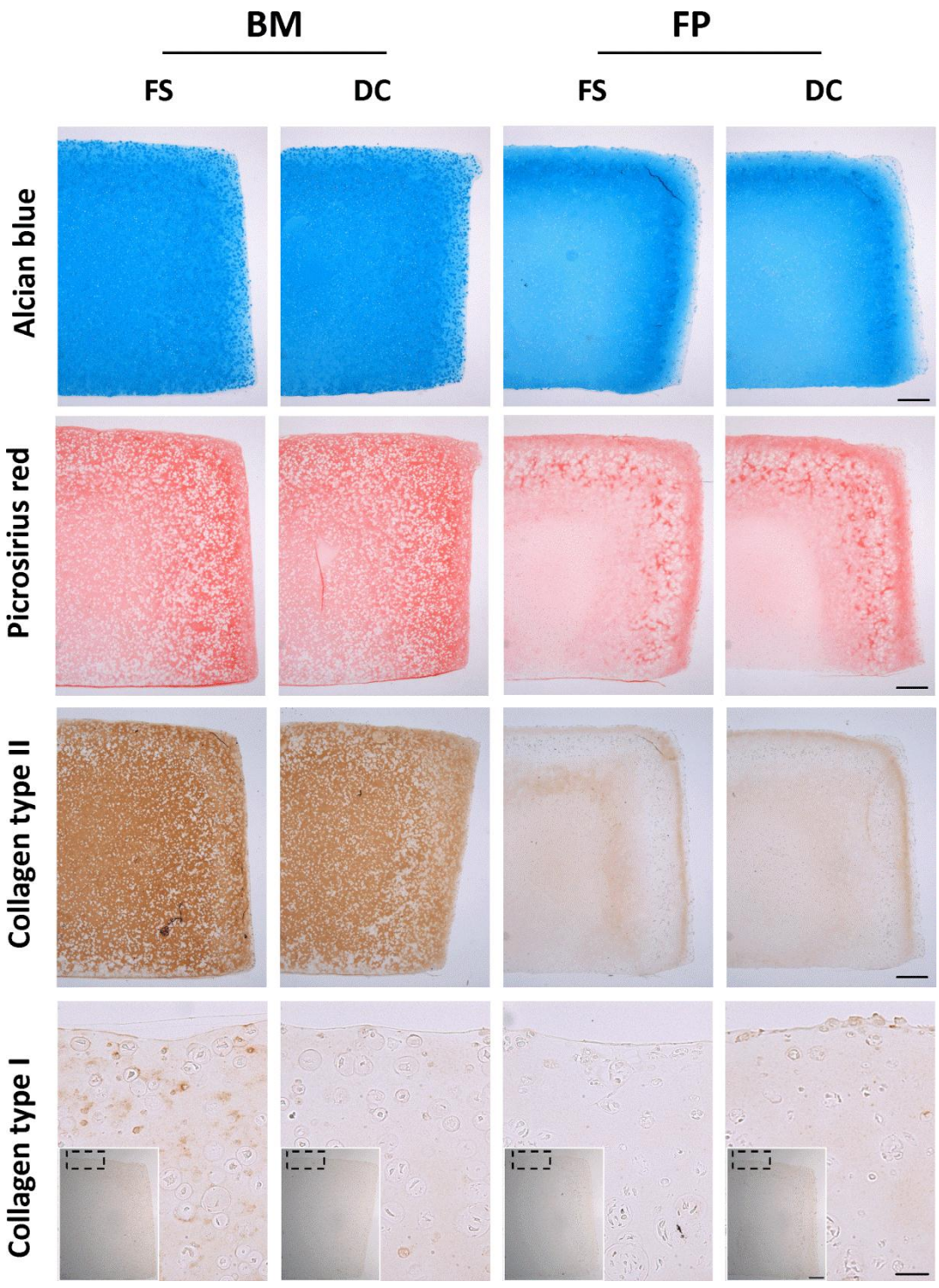

Supplementary Figure 3. Histological and immunohistological staining of BM and FP constructs, engineered using donor 2, in FS and DC culture at day 42. Scale bar in alcian blue, picrosirius red and collagen type II staining: 500 µm. Scale bar in collagen type I staining: 50 µm. Inserted images were taken at a low magnification to show staining at a bulk construct level, with box regions indicating area from where high magnification images were taken. Scale bar in inserted image: 500 µm.

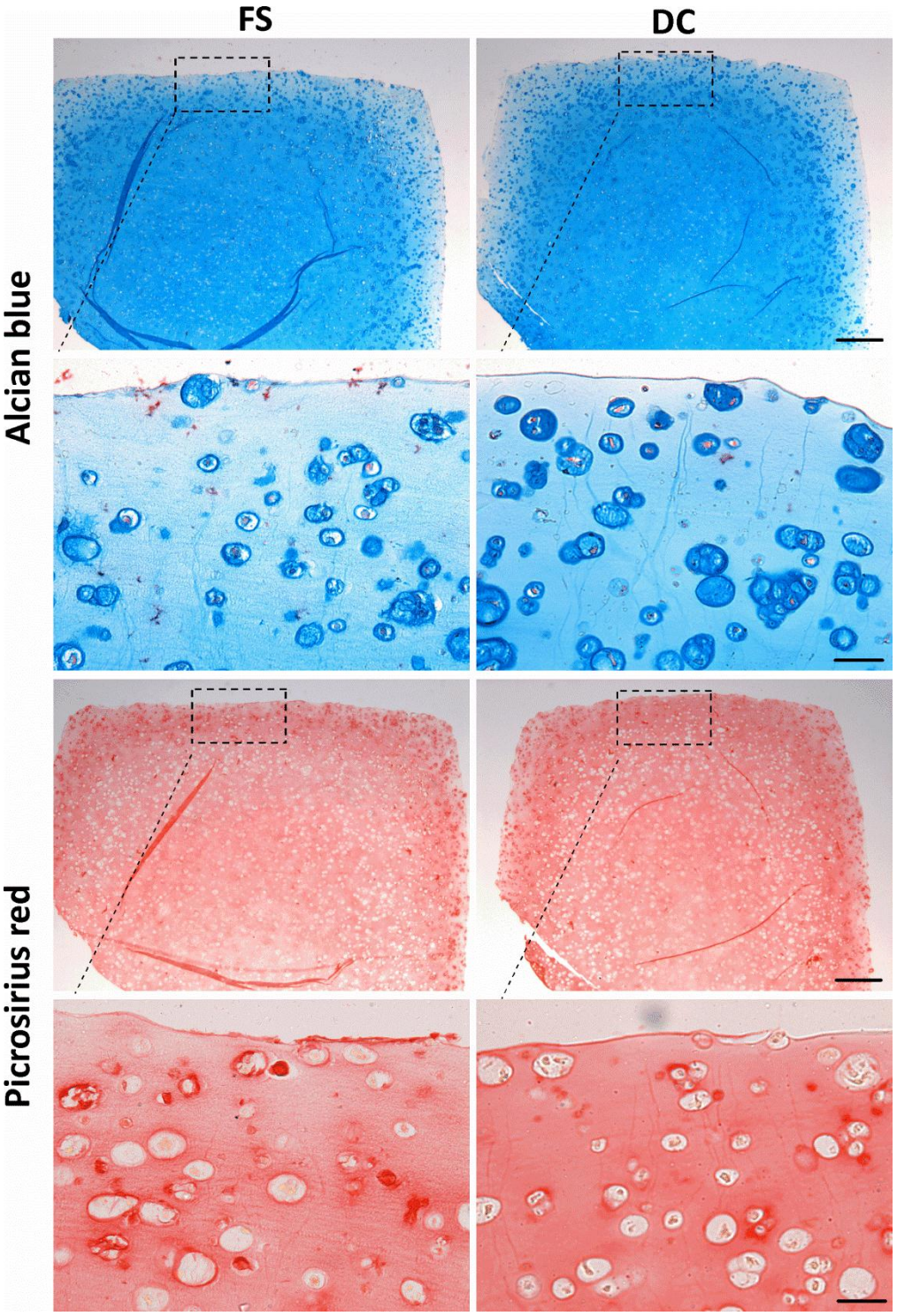

Supplementary Figure 4. Alcian blue and picrosirius red staining at the peripheral region of BM constructs in FS and DC culture at day 42. Images in first and third row were taken at a low magnification, showing staining at a bulk construct level; scale bar: 500 µm. Images in second and fourth row were taken at a high magnification, showing staining at the peripheral region of the constructs; scale bar: 50 µm.